MODULAR DESIGN OF STENT POLYMERS REGULATES HUMAN CORONARY ARTERY CELL TYPE-SPECIFIC OXIDATIVE RESPONSE AND PHENOTYPE

By

Spencer William Crowder

Thesis

Submitted to the Faculty of the

Graduate School of Vanderbilt University

in partial fulfillment of the requirements

for the degree of

MASTER OF SCIENCE

in

Biomedical Engineering

May, 2011

Nashville, Tennessee

Approved:

Dr. Hak-Joon Sung

Dr. Craig L. Duvall

ACKNOWLEDGEMENTS

First and foremost, I would like to thank Dr. Hak-Joon Sung for his guidance, advice, insight, and support throughout the last two years. Additionally, I thank Dr. Craig L. Duvall for his input on my work as well as his feedback and insight. I would like to thank my fellow lab members, Mukesh Gupta, Angela Zachman, Dae Kwang Jung, and Lucas Hofmeister, for their contributions to this work as well as their day-to-day support. My undergraduate assistants, Chad Augusty, Amanda Palmer and Yi Liang, have been crucial to completing this work and I appreciate all that they have done. I would like to thank Dr. Scott Guelcher and his advisee Elizabeth Adolph for allowing me to access, and also assisting me with, dynamic mechanical analysis. Finally, I would like to recognize the Vanderbilt Institute for Nanoscale Science and Engineering for training and access of their characterization instruments. This work was supported by NIH HL091465 and NSF 1006558

Most importantly I would like to thank my family for their continued support of my work, aspirations, and visions. Without them I would never have accomplished this work. They have shaped me throughout my entire life and the person I am today is a direct result of the love, dedication, and unequivocal encouragement with which they provide me every single day.

TABLE OF CONTENTS

Page

LIST OF TABLES

LIST OF FIGURES

CHAPTER I

INTRODUCTION

Copolymerization Techniques

The physicochemical and mechanical properties of biomaterials modulate the response of the cells and tissues with which they interact [1-4]. In particular, polymers can be designed to control cell activity and fate through structure-function relationships [4]. Copolymerization techniques provide a means for tuning polymer properties by incorporating subunits with different characteristics and varying their molar ratios, thereby controlling micro and macro structures [4]. By understanding the effect of each subunit on the resulting polymer properties, as well as the ability of each subunit to modulate a cellular response, polymer properties can be precisely optimized to control a specific biological function.

Coronary Stent Background

Implantation of a vascular stent is crucial to reduce human morbidity and mortality resulting from a vascular disease-induced, localized blood flow constriction [5]. The evolution of stent materials has included bare metal stents, polymers, and drug eluting stents, yet each of these technologies poses a specific set of issues that has prevented its widespread clinical translation. For example, bare metal stents cause restenosis and require additional surgery for removal, polymer byproducts can stimulate an inflammatory response, and drug eluting stents promote late thrombosis resulting from delayed re-

endothelialization [5, 6]. Therefore, much attention has been recently paid to design instructive, bioactive, bioresorbable materials as a solution to problems associated with classical treatments [7]. The ideal properties of a stent material include sufficient mechanical strength, moderate degradation kinetics, resorbable byproducts, and regulation of cellular activities (i.e., proliferation, viability), all of which can be precisely controlled by understanding how polymer structure affects the subsequent cellular response.

CHAPTER II

MODULAR DESIGN OF STENT POLYMERS REGULATES HUMAN CORONARY ARTERY CELL TYPE-SPECIFIC OXIDATIVE RESPONSE AND PHENOTYPE

Introduction

In this study, we have developed a new class of copolymers with tunable mechanical and chemical properties for coronary stent applications. Three subunits were copolymerized at varying molar ratios: poly(ε-caprolactone) (PCL) is a slow degrading, hydrophobic, highly biocompatible polymer that has been used in various biomedical applications [2, 8, 9]; poly(ethylene glycol) (PEG) is a hydrophilic polyether that can influence surface chemistry related to anti-adhesion of proteins and cells [10], bulk and degradation properties [11, 12] and oxidative activity [3, 4]; and, carboxyl PCL (cPCL) which carries a negative charge that improves hydrophilicity, can counteract repellent effects of PEG, and provides a site for functionalization of bioactive molecules to the polymer backbone [13]. A representative library of copolymers was synthesized and characterized, and thin film samples were prepared as culture substrates for primary human coronary artery smooth muscle cells (HCASMCs) and endothelial cells (HCAECs) to evaluate the applicability of these polymers for use as a coronary stent material. We investigated changes of phenotype and cellular activities of HCASMCs and HCAECs which are related to reactive oxygen

species (ROS)-mediated processes, as well as possible structure–function relationships of test materials in terms of their ability to modulate ROS activities. As a result, we identified the material properties that promoted the vascular homeostasis, balanced redox activities, and physiologically-relevant proliferation rates of both cell types. This structure-function relationship provides an insight into effective methods for outside-in control of healthy vascular cell function and specific material properties to reduce the pathological response that has been problematic in coronary stent applications.

Methods

Polymer Synthesis and Test Substrate Preparation

Poly(ethylene glycol) (PEG, Mw = 5000) was purchased from Sigma Aldrich (St. Louis, MO). Poly(ε-caprolactone) (PCL) homopolymer as well as PEG, PCL, and carboxyl-PCL (cPCL) were co-polymerized according to methods previously described[13-15] (Fig.1A). Copolymers of *x* mol % PEG, *y* mol % PCL, and *z* mol % cPCL were identified as *x*%PEG-*b*-*y%*PCL-*co*-*z*%cPCL where PEG-PCL is a block copolymer but cPCL addition is random within the PCL subunit. The polymers are abbreviated *x*%PEG-*y*%PCL-*z*%cPCL.

For testing mechanical and thermal properties, solvent cast films were prepared at 5% weight/volume (w/v) in dichloromethane in a 100mm glass Petri dish, left at room temperature in air overnight, and then placed under vacuum to remove excess solvent. For biological experiments, cover glass samples were prepared by spin coating (WS-650SZ-6NPP/Lite Spin Coater, Laurell Technologies, North Wales, PA) at 1% w/v in 70/30 chloroform/

dimethylformamide onto 15mm glass cover slips at 4,000 RPM for 30 seconds. Samples were placed under vacuum for at least two days before use. Samples for cellular interaction experiments were sterilized under UV light for 1 hour.

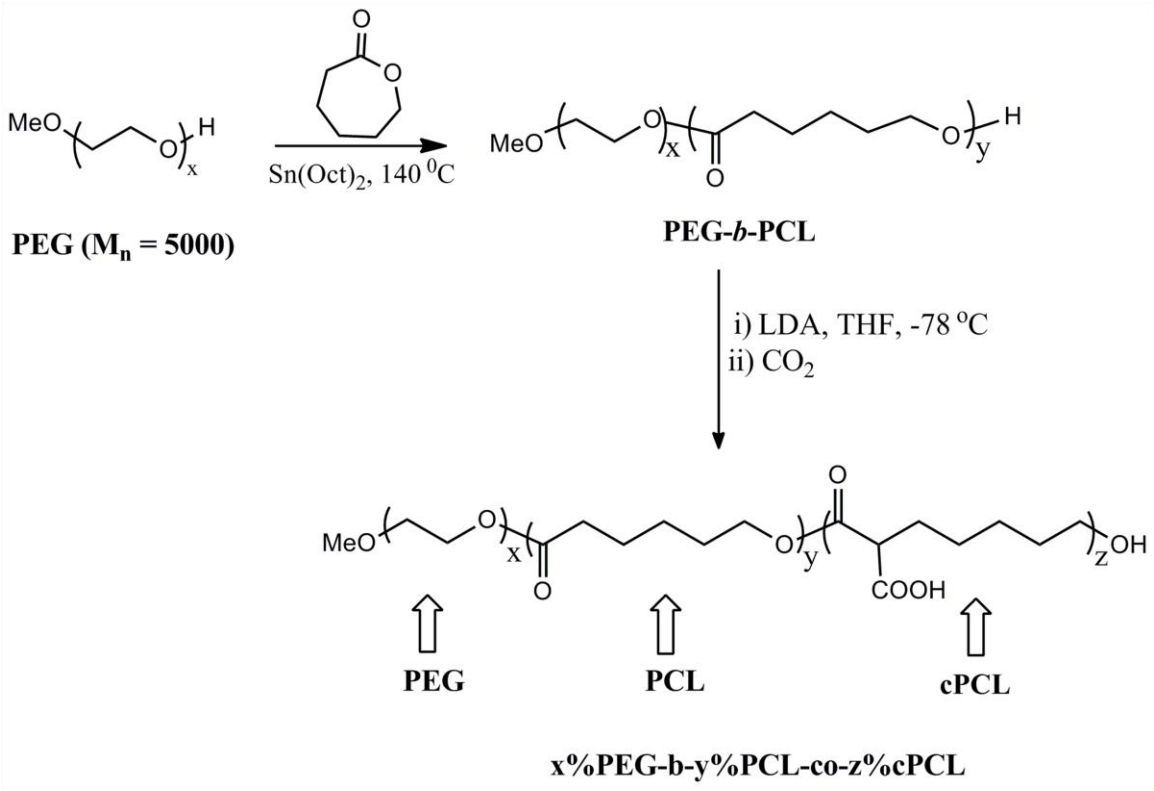

Figure 1. Polymers synthesis. Schematic representation of polymer synthesis. The random copolymer is identified as x%PEG-b-y%PCL-co-z%cPCL where x, y, and z represent the respective molar ratio. PCL-PEG is a block copolymer, but the addition of cPCL is random within the PCL subunit. The polymers are abbreviated x%PEG-y%PCL-z%cPCL.

Thermal and Mechanical Properties

Differential scanning calorimetry (DSC, Q1000, TA Instruments, New Castle, DE) was performed with sample mass between 5 and 10 mg in aluminum pans with tops. The procedure included two runs from -80°C to 100°C with a ramp rate of 10°C/minute. The values from the second run were reported such that thermal history was erased (n = 3). Thermogravimetric analysis (TGA-1000,

Instrument Specialist Inc., Twin Lakes, WI) was performed using a heating rate of20 ^{o}C/min to a final temperature of 600 ^{o}C.

Dynamic mechanical analysis (DMA, Q800 DMA, TA Instruments, New Castle, DE) was performed with samples that were soaked in dH_2O at 37°C for 2 days prior to testing. Wet stress and strain were recorded using a submersion clamp containing dH_2O at room temperature. A preload force of 0.1 N was applied to each sample and force was increased at a rate of 0.1 N/minute until failure. The average Young's Modulus was measured (n = 3). For temperature sweeps, a tension clamp was used with dry samples in air. The procedure included two runs from -80°C to 50°C with a ramp rate of 20 °C/minute and a strain of 30μm at 1Hz. All values were calculated using Universal Analysis software provided by TA Instruments.

Molecular Weight and Degradation

Gel permeation chromatography (GPC, Shimadzu Corp., Kyoto, Japan) with an inline Wyatt miniDAWN TREOS light scattering detector (Wyatt Technology Corp., Santa Barabara, CA) was used to measure M_n based upon dn/dC for each polymer type (n=4). Degradation properties of polymers were characterized by measuring M_n over time (i.e., 0, 4, 7, and 28 days) after incubation of polymer samples in phosphate buffer saline (PBS) at 37°C.

Surface Chemical Properties

The sessile drop method was used to measure contact angle with an in-house goniometer. One 10 µL drop of dH_2O was placed on each solvent-cast film, pictures were taken immediately, and the angles on both sides of the drop were measured to represent “dry” contact angles. Samples were then incubated with dH_2O drops for 2 hours at 37°C and measurements were taken to represent “wet” contact angles. All contact angles were analyzed through imaging and image analysis using ImageJ software (National Institutes of Health, Bethesda, MD) (n = 3).

In order to characterize the negative surface charge driven by free carboxyl groups of cPCL, polymer-coated cover glasses were incubated with 1% v/v carboxylate-terminated, fluorescence-conjugated polystyrene microspheres (Sigma) in water overnight at 37°C. Carboxyl groups generate a negative charge on the microsphere surface and microspheres are therefore repelled more by the polymer surface as cPCL % increases. Test samples were washed three times to remove repelled microspheres from the test surfaces and the fluorescence intensity of remaining microspheres on the test sample was measured with a plate reader (infinite F500, Tecan Group Ltd., Mannedorf, Switzerland) (n = 4).

Cell Culture

Human coronary artery vascular smooth muscle cells (HCASMCs, passages 6-8) were cultured in Dulbecco’s Modified Eagle’s Medium (DMEM, Gibco Cell Culture, Carlsbad, CA) supplemented with10% heat-inactivated fetal

bovine serum (FBS, Gibco), 1% penicillin-streptomycin (Gibco), and 1% L-glutamine (Gibco). Human coronary artery endothelial cells (HCAECs, passage 7) were cultured in MesoEndo Growth Medium (Cell Applications, Inc., San Diego, CA) supplemented with 10% FBS and 1% penicillin-streptomycin. Cells were purchased from Cell Applications, Inc. (San Diego, CA). Cells were cultured for three days on test polymer samples before end point experiments.

Immunofluorescence Staining

Cells were fixed in 4% paraformaldehyde (Sigma) in dH_2O and incubated with primary antibody (1:100) overnight at 4°C. To measure proliferation, cells were incubated with 5-bromo-2'-deoxyuridine (BrdU, Sigma) at 20 μM for 16 hours. Incorporated BrdU in proliferating cells were detected by staining with primary rat anti-human BrdU antibodies (Abcam, Cambridge, MA), followed by addition of secondary DyLight594-conjugated goat anti-rat (Jackson Immunoresearch, West Grove, PA) antibodies. To evaluate a healthy contractile phenotype in HCASMCs expression of smooth muscle myosin heavy chain (smMHC) was detected by staining with primary mouse anti-human smMHC antibodies (Abcam), followed by addition of secondary TRITC-conjugated goat anti-mouse (Abcam) antibodies. To evaluate inflammatory action of HCAECs, expression of vascular cell adhesion molecule (VCAM)-1 was detected by staining with APC-conjugated anti-human VCAM-1 antibodies (CD 106, BioLegend, San Diego, CA). Cell nuclei were counterstained with Hoechst 33258 (Sigma) in all the aforementioned types of fluorescence staining. Cells

were imaged under a Nikon Eclipse Ti inverted fluorescence microscope (Nikon Instruments Inc, Melville, NY). Relative protein expression was quantified by measuring fluorescence intensity from antibody staining, which was normalized to cell number from Hoechst nucleus staining using ImageJ. Cell proliferation was presented by the percent of BrdU-positive cells in the total number of cells (%) (n=12 pictures/polymer).

Cell Activities

To measure intracellular superoxide and hydrogel peroxide, cells were incubated with dihydroethidium (DHE, Invitrogen) and dichlorofluorescein diacetate (DCFDA, Invitrogen), respectively for 30 minutes at 5 μg/mL following the previously reported method [4]. To measure cell viability, cells were stained with Calcein AM (Invitrogen, 1 μg/mL). All cells were counterstained with Hoechst nucleus staining (5 μg/mL) to measure the total number of cells. Fluorescence intensity of each staining (i.e., DHE, DCFDA, and Calcein AM) was measured with a plate reader (Tecan) and were normalized to the corresponding cell number. To measure total protein content, cells were lysed, proteins were harvested and quantified by a colorimetric assay (BioRad, Hercules, CA). For morphological analysis, HCASMC were stained with Texas Red-X phalloidin (Invitrogen) and cell circularity was measured using ImageJ (n = 80) [16]. Degree of circularity is a 0-10 scale defined as 0 being an elongated morphology and 10 representing a perfect circle.

Statistical Analysis

In all experiments, results are presented as means ± standard error mean (SEM). Comparisons between individual sample groups were performed using an unpaired Student's t-test. For all statistics, $p < 0.05$ was considered statistically significant.

Results

Synthesis

A subset of six polymers were synthesized, characterized and evaluated for cellular interaction: 100%PCL, 4%PEG-96%PCL, 8%PEG-92%PCL, 4%PEG-86%PCL-10%cPCL, and 8%PEG-82%PCL-10%cPCL. PCL polymers were synthesized by ring-opening polymerization and, in the case of copolymers, were extended from PEG (Fig. 1A). Terpolymers (e.g. polymers containing all three subunits) were synthesized according to the method reported previously [13], but with x%PEG-*b*-y%PCL as the starting material. M_n values ranged from 60 – 140kDa, as determined by GPC.

Degradation

M_n was measured by GPC following incubation of each polymer sample in PBS at 37℃ at the indicated time points over 28 days. The M_n of 100%PCL decreased by ~13% at 28 days post incubation (Fig. 1B). With the addition of 10%cPCL to the PCL homopolymer (i.e., 90%PCL-10%cPCL), the polymer degraded more quickly (~19%) and this effect was enhanced (~25%) upon

addition of the hydrophilic 4% PEG subunit (i.e. 4%PEG-90%PCL-10%cPCL), suggesting the effect of hydrophilic cPCL and PEG on hydrolysis of ester bonds in the test polymers (Table 1).

Number-average molecular weight (M_n)

Polymer Composition	Day 0 (kDa)	Day 4 (kDa)	Day 7 (kDa)	Day 28 (kDa)	% M_n Remaining
100%PCL	93.2	86.9	84.1	80.7	86.6%
90%PCL-10%cPCL	139.1	135.7	133.2	112.4	80.8%
4%PEG-86%PCL-10%cPCL	95.3	92.2	85.7	71.3	74.8%

Table 1. Degradation of test polymers. Degradation results for three representative test polymers. Values were obtained by GPC using light scattering dn/dC measurements and represent the average of four M_n measurements. Percent remaining represents the M_n at day 28 relative to the initial value.

Thermal Properties

Thermal degradation of each polymer sample was first evaluated by TGA. The results reveal stability of all polymers up to 200 °C, supporting their use in physiological applications (Fig. 2A). DSC was then used to monitor changes in the thermal properties of different polymer composition (Fig. 2B). The enthalpy change (ΔH) and melting temperature (T_m) of 100%PEG was higher than those of 100%PCL. Therefore, compared to 100%PCL, ΔH and T_m increased upon addition of PEG to the PCL homopolymer (i.e., 4%PEG-96%PCL and 8%PEG-92%PCL), but decreased with cPCL (i.e., 90%PCL-10%cPCL) (Fig. 2B). Interestingly, addition of both PEG and CPCL in the terpolymers (i.e., 4%PEG-86%PCL-10%cPCL and 8%PEG-82%PCL-10%cPCL) dramatically decreased ΔH and T_m, compared to the test homo- and copolymers. Also ΔH and T_m increased as the PEG content increased from 4% to 8% in the test terpolymers. The DMA result showed that the wet glass transition temperature (Wet T_g)

decreased as the PEG and/or the cPCL content(s) increased in the test polymer types (Table 1). In particular, in the test terpolymers, the addition of cPCL amplified the PEG effect, resulting in a reduction of Wet T_g, compared to PEG-PCL copolymers.

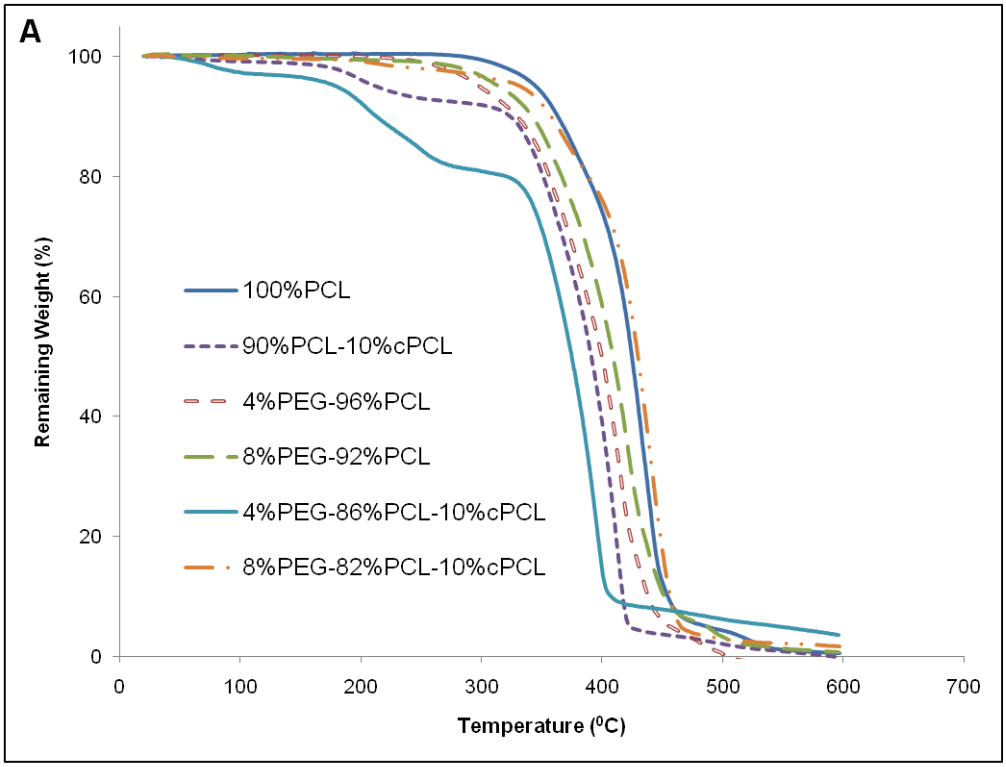

B

Polymer Composition	ΔH (J/g)	T_m (°C)
100%PCL	79.24	58.01
90%PCL-10%cPCL	73.68	57.82
4%PEG-96%PCL	82.21	57.28
8%PEG-92%PCL	91.26	58.06
4%PEG-86%PCL-10%cPCL	58.12	57.00
8%PEG-82%PCL-10%cPCL	70.97	57.14
100%PEG	216.67	60.47

Figure 2. Thermal properties of dry polymers. (a) Thermogravimetric analysis and **(b)** differential scanning calorimetry (DSC) of dry polymer samples. Enthalpy change (ΔH) and melting temperature (T_m) were obtained from the second heating curve and represent the average of three measurements (n = 3).

Polymer Composition	Wet T_g (°C)	Wet E (MPa)	Wet σ_U (MPa)
100%PCL	-57.54	232.6 ± 49.6	14.6 ± 3.4
90%PCL-10%cPCL	-58.08	122.4 ± 49.4	7.0 ± 2.5
4%PEG-96%PCL	-57.91	145.6 ± 44.8	11.9 ± 3.3
8%PEG-92%PCL	-59.64	178.0 ± 47.3	13.0 ± 4.0
4%PEG-86%PCL-10%cPCL	-59.80	43.6 ± 2.9	2.4 ± 0.6
8%PEG-82%PCL-10%cPCL	-59.40	11.9 ± 4.1	0.6 ± 0.3

Table 2. Mechanical and thermal properties of wet polymers. Wet glass transition temperature (T_g), wet Young's modulus (E), and wet ultimate tensile stress (σ_U) were obtained with dynamic mechanical analysis (DMA) using solvent casted film samples incubated in dH_2O for two davs at 37 °C.

Wet Mechanical Properties

DMA was used to evaluate the wet mechanical properties of the test polymers. Solvent-cast films were incubated in dH_2O for 2 days at 37°C prior to testing to investigate the hydrophilic effects of PEG and cPCL on a mechanical property in a wet condition. Upon addition of cPCL (i.e., 90%PCL-10%cPCL), the wet Young's modulus (E) and ultimate tensile strength (σ_U) decreased, compared to 100%PCL (Table 1). Addition of PEG (i.e., 4%PEG-96%PCL and 8%PEG-92%PCL) also decreased these parameters compared to 100%PCL, but to a lesser extent than 90%PCL-10%cPCL. In terpolymers, addition of both PEG and cPCL dramatically reduced E and σ_U, compared to the test homo- and copolymers, indicating the combined effects of PEG and cPCL on the mechanical properties.

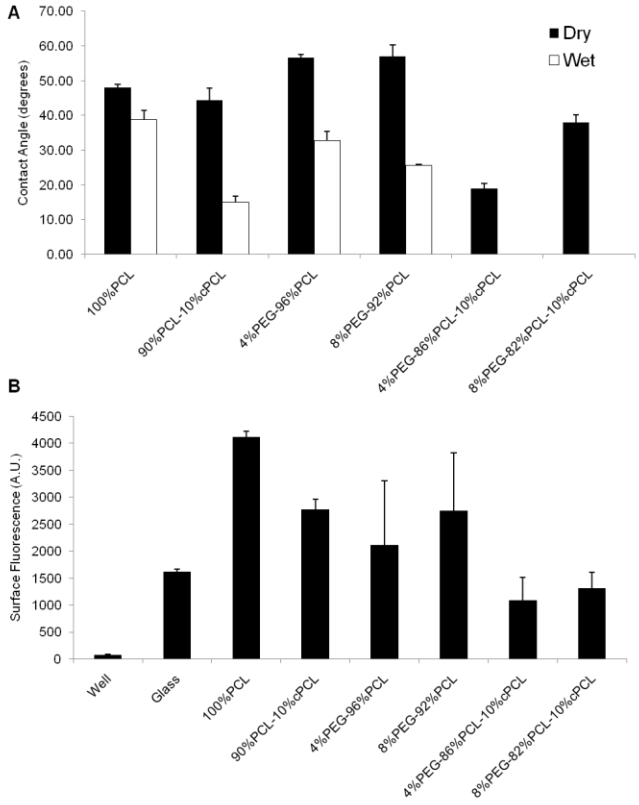

Figure 3. Surface chemistry. (a) Advancing contact angle analysis for dry and wet polymer film surfaces (n=3). Wet polymer samples were incubated with one drop of dH_2O for 2 hours at 37°C. **(b)** Polymer-coated glass cover slips were incubated with carboxylate-terminated, fluorescence-conjugated polystyrene microspheres to evaluate surface chemistry. Negative surfaces exhibit a lower fluorescence signal due to charge repulsion (n = 4).

Water Contact Angle and Surface Charge

Using the sessile drop method, water contact angle was assessed to evaluate the ability of PEG and cPCL subunits to modulate surface hydrophilicity (Fig. 3A). The “dry” sessile contact angle was not significantly different among the test polymer types. Following incubation for 2 hours at 37 °C with 95% humidity, contact angles decreased noticeably, compared to dry sessile contact angles. In particular, the “wet” contact angle decreased as the cPCL and/or PEG content increased in the test polymer types, indicating the contributions of the PEG and cPCL hydrophilic subunits. The wet contact angles were 0° on the test terpolymers, indicating that the test surfaces fully absorbed the drop.

Relative negative surface charge was evaluated by employing the concept of charge-charge repulsion between free carboxyl groups on microspheres and

the polymer surface. A strong fluorescence intensity indicates a surface with a low negative charge due to reduced charge-charge repulsion. The relative fluorescence intensity of polymer-coated cover glass was measured following overnight incubation with carboxylate-terminated fluorescent microspheres (Fig. 3B). The 100%PCL surface exhibited the highest fluorescence intensity, indicating the least negative charge. The addition of cPCL reduced the fluorescence intensity significantly, as compared to the test polymers that do not contain cPCL, confirming the presence of surface charge derived from cPCL. The lowest fluorescence intensities were observed for the test terpolymers, indicating an additional repellent effect of PEG.

Cellular Interaction

- HCASMC Response

To determine the optimum composition of polymers for coronary stent applications, responses of HCASMCs to test polymers were investigated first. Balance of cellular oxidative mechanisms is crucial for maintaining vascular homeostasis and preventing pathogenesis [17-21]. Therefore, we measured intracellular reactive oxygen species (ROS) levels, specifically superoxide ($O_2^{\bullet-}$) and hydrogen peroxide (H_2O_2), and found them to vary significantly between test polymer types (Fig. 4A-B). Intracellular $O_2^{\bullet-}$ levels correlated inversely with intracellular H_2O_2 levels except in the case of 4%PEG-96%PCL (Fig. 4A). For example, 8%PEG-92%PCL displayed a low level of $O_2^{\bullet-}$, but a high level of H_2O_2; conversely, terpolymer test samples displayed the highest levels of $O_2^{\bullet-}$ and the

lowest levels of H_2O_2. In the test co- and terpolymers, increasing PEG molar ratios resulted in higher intracellular H_2O_2 levels, but this effect was counteracted by the addition of negatively-charged cPCL (Fig. 4B). HCASMCs grown on the test terpolymers showed statistically significant differences in both H_2O_2 and $O_2^{\bullet-}$ levels relative to other test copolymers ($p < 0.05$).

HCAMSCs in all polymer groups maintained viability (> 70%), but proliferation varied significantly (Fig. 4C-D). Percentages of proliferating HCASMCs correlated proportionally with total protein contents for each group (Fig. 4d-e), indicating that protein synthesis is required for cells to undergo proliferation. Cells grown on terpolymers resulted in significantly different percentages of proliferation and total protein content ($p < 0.05$). Interestingly, proliferation percentages correlated inversely with intracellular H_2O_2 levels except in the case of 100%PCL (Fig. 4A).

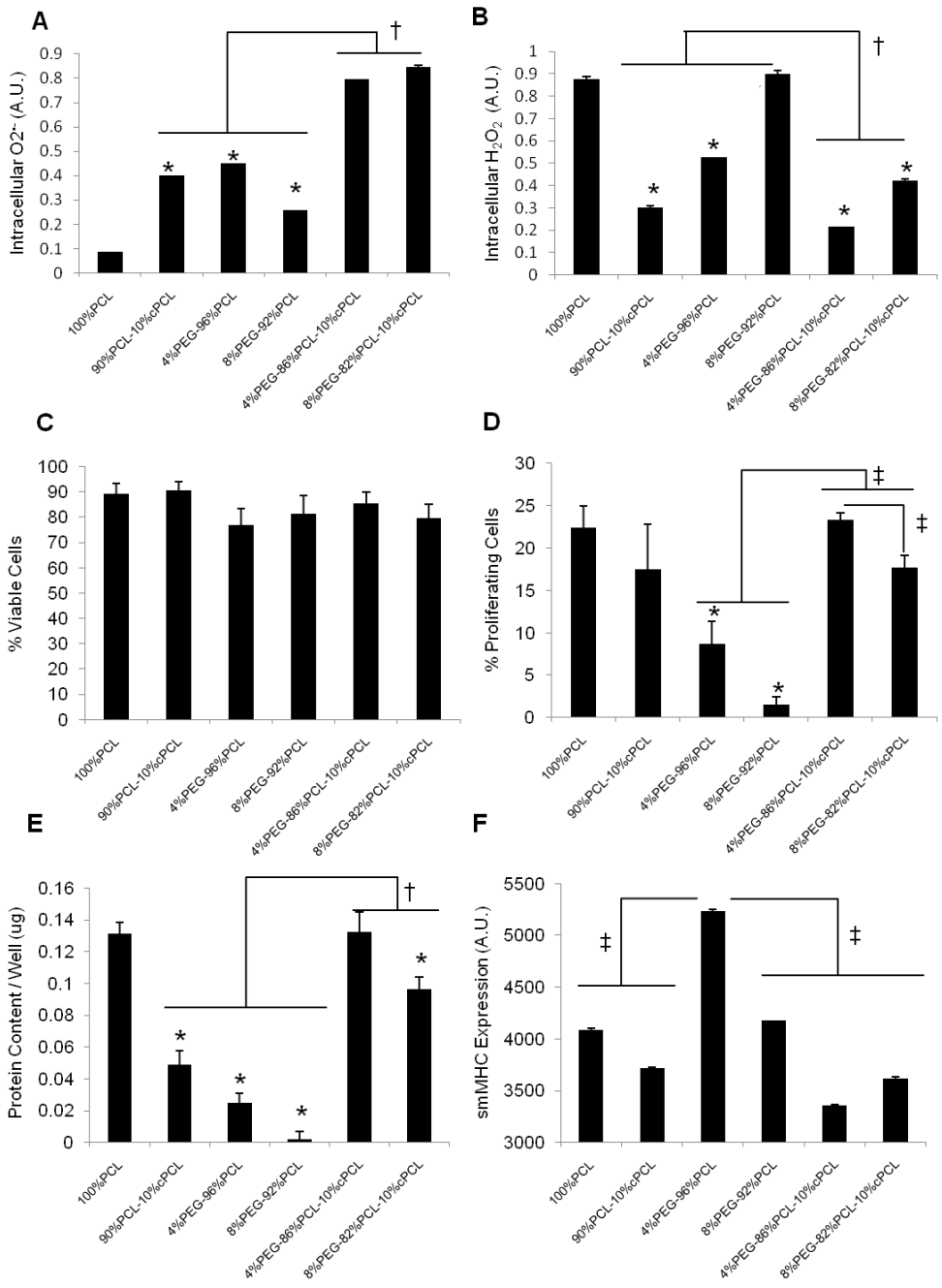

Figure 4. HCASMC interaction with polymers (a) Intracellular $O_2^{\bullet-}$ and **(b)** H_2O_2 measured by DHE and DCFDA, respectively. **(c)** Cell viability and **(d)** percent proliferating HCASMCs as determined by calcein and BrdU staining, respectively. **(e)** Total content of intracellular proteins and **(f)** smooth muscle myosin heavy chain (smMHC) expression. *$p < 0.01$ *vs.* 100%PCL; †$p < 0.05$ and ‡$p < 0.01$ between test materials indicated by the lines.

In general, healthy vascular SMCs proliferate at a very low rate and assume a contractile phenotype that is characterized by strong smMHC

expression, and a spindle-like morphology [22, 23]. In contrast, unhealthy, “dedifferentiated” SMCs assume a circular cobble stone-like, synthetic phenotype in which smMHC expression is significantly downregulated [22]. In order to test the ability of the different polymers to discourage a phathogenic, synthetic phenotype, we stained for smMHC and found that 4%PEG-96%PCL promoted a statistically greater level of smMHC expression in HCASMCs relative to all other conditions ($p < 0.01$, Fig. 4F). Additionally, HCASMC morphology was altered depending upon substrate composition (Fig. 5). Degree of circularity is a 0-10 scale defined as 0 being an elongated morphology and 10 representing a perfect circle. 100%PCL and 90%PCL-10%cPCL showed a slight trend towards a less circular morphology distribution. 4%PEG-96%PCL showed the most distinct peak for a low degree of circularity of all groups, supporting the highest smMHC expression of HCASMCs on this polymer. In contrast, 8%PEG-92%PCL showed the most distinct peak at a high degree of circularity. Interestingly, the increase in PEG molar ratio resulted in the two strongest morphological biases of all polymers tested, likely due to the ability of PEG to modulate protein adsorption and cell adhesion. The test terpolymers showed bimodal circularity distributions that represent the contributions from all three polymeric subunits: 100%PCL promotes slightly elongated morphologies, 90%PCL-10%cPCL promotes an even distribution of centered morphologies (degree of circularity ~5), and PEG-containing copolymers bias the cell morphology depending upon molar percentage (Fig. 5).

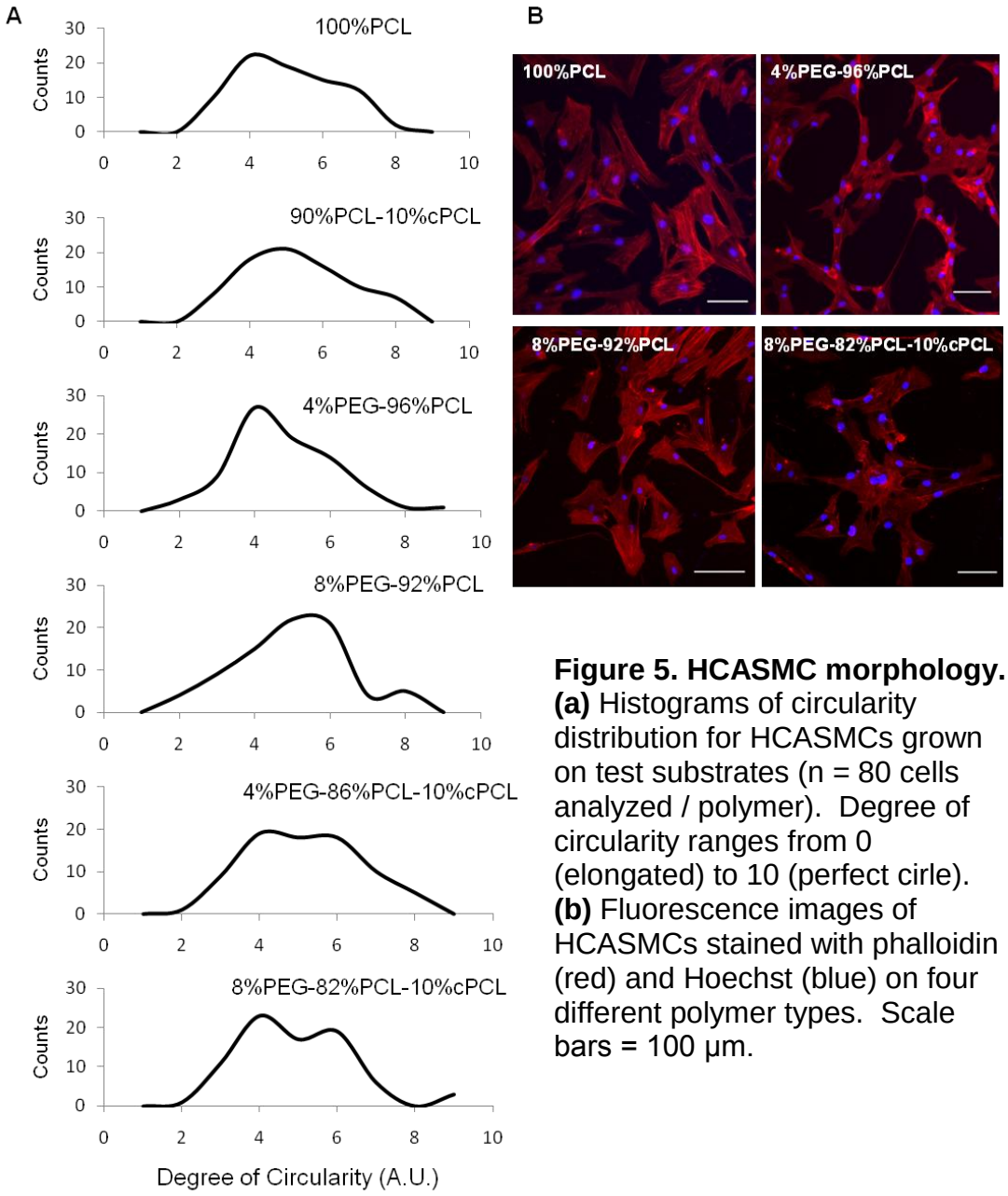

Figure 5. HCASMC morphology. **(a)** Histograms of circularity distribution for HCASMCs grown on test substrates (n = 80 cells analyzed / polymer). Degree of circularity ranges from 0 (elongated) to 10 (perfect cirle). **(b)** Fluorescence images of HCASMCs stained with phalloidin (red) and Hoechst (blue) on four different polymer types. Scale bars = 100 μm.

- HCAEC Response

We then evaluated the responses of HCAECs to test polymer substrates. Vascular smooth muscle cells and endothelial cells comprise the majority of the vasculature and understanding how polymer properties can modulate the response of each cell type differently is critical to designing a vascular stent

material that prevents restenosis (e.g., SMC growth, migration, and phenotype change) while enhancing re-endothelialization. Maintenance of homeostatic redox balance differs in endothelial [17, 24] and smooth muscles cells [20] and we found that trends in ROS levels of HCAECs were opposite to those of HCASMCs (Fig. 6A).

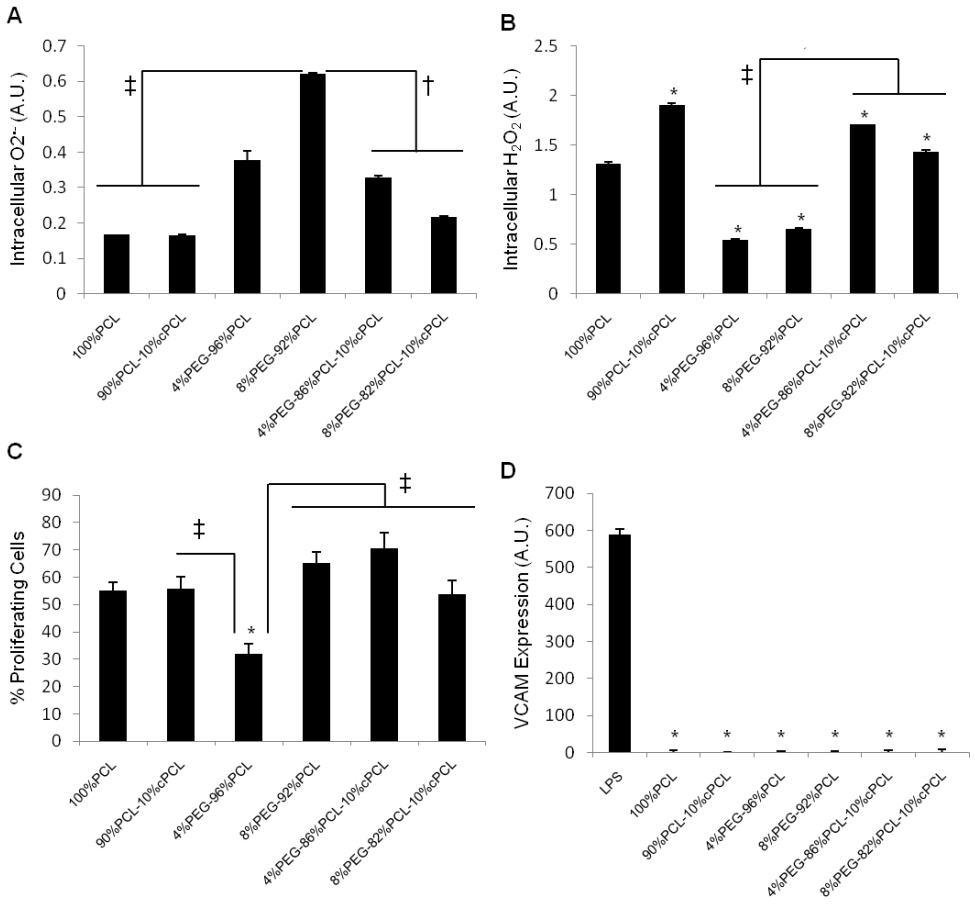

Figure 6. HCAEC interaction with polymers. **(a)** Intracellular $O2^{\bullet-}$ and **(b)** H_2O_2 measured by DHE and DCFDA, respectively. **(c)** Percent proliferating HCAECs as determined by BrdU staining. **(d)** Vascular cell adhesion molecule (VCAM) expression. *$p < 0.01$ *vs.* 100%PCL, †$p < 0.05$ and ‡$p < 0.01$ between test materials indicated by the lines.

The 8%PEG- 92%PCL copolymer exhibited a statistically higher level of $O2^{\bullet-}$ expression relative to all other groups except 4%PEG-96%PCL ($p < 0.01$, Fig.

6A). Intracellular H_2O_2 levels of HCAECs correlated inversely with $O2^{\bullet-}$(Fig. 6B), which was similar to the trends seen in HCASMCs (Fig. 4A and B). HCAEC proliferation was high (> 50%) in all groups except 4%PEG-96%PCL (20-30%), which was significantly lower than 100%PCL ($p < 0.01$) and all other groups ($p < 0.05$, Fig. 6C). To evaluate if any of the polymers stimulate pro-inflammatory activation of HCAECs, VCAM-1 expression of HCAECs was measured on test polymers. The condition with lipopolysaccharide (LPS) treatment was used as a control (Fig. 6D). VCAM-1 expression in ECs is stimulated by pathoglogical cues, resulting in recruitment of inflammatory cells but its expression is extremely low in normal ECs [25]. We found that none of the polymers stimulated VCAM expression, thereby further supporting their applicability as biocompatible cardiovascular biomaterials, in particular as vascular stent materials (Fig. 6D).

Discussion

The purpose of this study was to synthesize and characterize a new class of copolymers with tunable mechanical and physical properties for biomedical applications, particularly coronary artery stents. Poly(ε-caprolactone) (PCL) was used as the primary component due to its biocompatibility, hydrophobicity, and slow degradation rate [2, 8, 9, 26]; poly(ethylene glycol) (PEG) to promote hydrophilicity, water absorption and to modulate repulsion of proteins and cells [4]; and carboxyl-PCL (cPCL) for increased hydrophilicity and exposure of a negative surface charge that was found to reduce the repellent effect of PEG [4, 13]. The three subunits exhibit distinct characteristics and, when copolymerized

at varying molar ratios, the resulting polymer can be tailored to modulate cellular response. Investigations with two primary human vascular cell types revealed the structure-function relationships that control cell proliferation and phenotypic changes in a reactive-oxygen species (ROS)-dependent manner.

PCL is a semi-crystalline, hydrophobic polymer with slow degradation kinetics in aqueous environments [8, 9]. Addition of the random hydrophilic cPCL subunit or PEG block improved water absorption, facilitated hydrolytic cleavage, and resulted in a faster degradation rate (Fig. 1B). In dry conditions, adding cPCL reduced enthalpy change and melting temperature due to decreased chain regularity (Fig. 2B). Inclusion of the PEG block, however, increased these values by promoting chain packing and crystallinity, which is supported by the values for 100%PEG. In wet conditions, addition of either cPCL or PEG reduced glass transition temperature (T_g), Young's modulus (E), and ultimate tensile strength (σ_U) (Table 1). This effect was synergistically amplified in the test terpolymers due to the increased water absorption by the hydrophilic subunits which decreased crystallinity, weakened the overall polymer structure, and reduced mechanical properties. Additionally, polymer surfaces composed of increasing molar ratios of PEG and cPCL proportionally absorbed more water, as seen by contact angle (Fig. 3A). Surface charge analysis using carboxylate-terminated microspheres further confirmed these results (Fig. 3B). A decrease in fluorescence signal (i.e. more negative charge) was observed for test samples containing PEG and/or cPCL. The rise in fluorescence intensity for 8%PEG polymers relative to 4%PEG can be explained by the formation of hydrogen

bonds between the carboxylate-terminated microspheres and the dense block of ether groups at the surface [27, 28].

Homeostasis of vascular SMCs and endothelial cells (VEC) is dependent upon effective redox mechanisms [22]. Imbalances in ROS, such H_2O_2 and $O_2^{\bullet-}$, result in abnormal cell proliferation, changes in phenotype, and the progression of cardiovascular diseases, including hypertension, atherosclerosis, and restenosis [19, 21, 29, 30]. VSMCs and VECs produce ROS at a basal level that is crucial for cell signaling. However, excess ROS, either from intracellular production or those released by inflammatory cells in pathological states, have been implicated in disease progression, specifically causing the "dedifferentiation" of VSMCs [22] and hyperproliferation of VECs [17]. Interestingly, H_2O_2 and $O_2^{\bullet-}$ have been shown to stimulate opposite responses in VSMC and EC: VSMC proliferation is promoted by H_2O_2 and arrested by $O_2^{\bullet-}$ [20], but EC proliferation is stimulated by $O_2^{\bullet-}$ and arrested by H_2O_2 [17, 24]. Healthy VSMCs are differentiated, quiescent, and maintain a contractile phenotype, which is characterized by an elongated spindle-like morphology and expression of smMHC [18, 22]. However, unhealthy VSMCs dedifferentiate, proliferate, assume a synthetic phenotype, a circular morphology, and display low smMHC expression. Healthy VECs proliferate slowly *in vivo* and hyperproliferation of VECs can lead to vessel blockage [24, 31]. These competitive signaling events reveal a complex framework in which maintenance of two healthy cell types requires a specific ROS balance. We therefore investigated the role of these polymers in modulating intracellular ROS production, cell proliferation, and

phenotypic changes in HCASMCs and HCAECs, and identified structure-function relationships that provide healthy versus pathological environments.

As seen in Figure 4, HCASMC intracellular ROS varied dramatically in response to different polymer substrates. In most groups, a high level of $O_2^{\bullet-}$ correlated with a low level of H_2O_2, indicating the activity of superoxide dismutase (SOD) in converting $O_2^{\bullet-}$ to H_2O_2 [24]. PEG-containing substrates have been shown to promote intracellular H_2O_2 production, as seen for 4%PEG-96%PCL and 8%PEG-92%PCL (Fig. 4B) [3, 4]. In the test terpolymers, the addition of cPCL counteracted the effects of PEG and resulted in the lowest H_2O_2 levels. Although cells on all polymers maintained intact cell viability (Fig. 4C), differences in proliferation rates and total protein content reflect the ability of $O_2^{\bullet-}$ and H_2O_2 to promote and arrest HCASMC proliferation, respectively (Fig. 1D-E). In most groups, increasing levels of H_2O_2 corresponded with decreased proliferation rate and protein content whereas $O_2^{\bullet-}$ levels correlated with increased proliferation. However, HCASMC on 100%PCL showed high intracellular H_2O_2 and low intracellular $O_2^{\bullet-}$, yet maintained a high proliferation rate and protein content. Because this is the only purely hydrophobic substrate, we believe that the cell adhesive surface of hydrophobic 100%PCL promoted proliferation of this mesenchymal cell type and that this effect was more influential than the competing ROS-induced arrest of proliferation [2].

Expression of smMHC was statistically higher in HCASMCs grown on 4%PEG-96%PCL relative to all other groups (Fig. 4F). Morphological analysis revealed that cells on 4%PEG-96%PCL showed the strongest bias towards an

elongated spindle-like phenotype, which is a typical phenotype of healthy HCASMCs (Fig. 5). Interestingly, in these cells, both intracellular ROS types stayed within a moderate range that, along with strong smMHC expression, suggests an effective redox balance that maintained a healthy contractile phenotype. In contrast, cells grown on the test terpolymer substrates displayed high levels of intracellular $O_2^{\bullet-}$ coupled with sustained proliferation rates and the lowest levels of smMHC expression in HCASMCs. Cell circularity of HCASMCs on the test terpolymers assumed a bimodal distribution, suggesting a heterogeneous population of contractile and synthetic phenotypes on these surfaces (Fig. 5). HCAMSCs on 8%PEG-92%PCL had high intracellular H_2O_2 and reduced proliferation, but low protein content (Fig. 4B-D), indicating that the repellent effect of PEG prevented cell attachment and cell-matrix interaction. Together these results indicate that 4%PEG-96%PCL is the most appropriate substrate to maintain a healthy HCASMC phenotype, as characterized by strong smMHC expression, a low proliferation rate, and an effective redox balance.

We then assessed the response of HCAEC on polymer substrates in order to understand how the different polymeric subunits can influence the two cell types differently. By monitoring the response of two complementary coronary artery cell types, we can identify the most appropriate polymer(s) for a coronary stent application. We found that trends in intracellular ROS levels of HCAEC were opposite to those of HCASMC with respect to the substrate composition (Fig. 6A-B). Intracellular H_2O_2 was minimized on 4%PEG-96%PCL and 8%PEG-92%PCL whereas intracellular $O_2^{\bullet-}$ was increased. HCAECs on the test

terpolymers displayed high levels of $O_2^{\bullet-}$ and low levels of H_2O_2. Proliferation rates agreed with intracellular ROS patterns except for HCAECs on 8%PEG-92%PCL, which displayed high intracellular $O_2^{\bullet-}$ and low H_2O_2, but maintained a high proliferation rate (~65%). As with HCASMC, the 8%PEG-92%PCL exhibited a strong repellent effect that prevented cell-matrix interactions, but for HCAECs, the dominant cell-cell interactions promoted proliferation in an ROS-independent manner. HCAECs grown on all polymers except 4%PEG-96%PCL showed proliferation rates in a pathophysiological range (>40%), making them less ideal for cardiovascular application. Due to intermediate production of ROS and maintenance of a physiologically-relevant proliferation rate, 4%PEG-96%PCL is the most appropriate material for applications that require contacts with HCAECs *in vivo*.

Polymer substrates were shown to modulate cellular activity in an ROS-dependent manner. Analysis of the relationships between polymer properties and the subsequent cellular response revealed structure-function relationships that may provide insight into manipulating cellular activities by exploiting specific polymer characteristics. Intracellular H_2O_2 in HCASMCs followed the same trend as the polymer mechanical properties (e.g. E and σ_U) whereas intracellular $O_2^{\bullet-}$ followed the same trend as the surface charge. We believe that increased surface charge stimulates outside-in transport of $O_2^{\bullet-}$ that results in an abundance of intracellular $O_2^{\bullet-}$. Because production of H_2O_2 reflects HCASMC proliferation potential and HCASMC are normally quiescent , stiffer substrates likely resemble a pathophysiological environment that promotes proliferation, such as that found

in atherosclerosis [32]. For interactions with HCASMC, 4%PEG-96%PCL provided the best substrate because of its moderate surface charge and mechanical properties, as well as promotion of a balanced ROS production. This combination of properties promoted a healthy, contractile phenotype. Cellular behavior can also be modulated by PEG domains at the polymer surface, such as with 8%PEG-92%PCL. The HCASMC from the mesenchymal lineage are cell-matrix interactive and did not grow well on this substrate; however, the HCAEC from the endothelial lineage are cell-cell interactive and flourished. Both of these results disagreed with the trends of all other groups and therefore provide an interesting insight to control competitive cell-cell versus cell-matrix interactions.

Conclusion

In this study, we have synthesized and characterized a new class of copolymers with tunable properties for biomedical applications. Polymer properties are influenced by the molar ratios of the individual subunits and, by varying their specific contributions, the resulting bulk and surface properties can be controlled. Investigations of the responses of two primary human coronary artery cell types revealed an ability of the substrate to modulate intracellular reactive oxygen species, which directed changes in phenotype and related cellular activities of the test cell types. Our study indicates that the polymer composition-dependent material properties can directly influence cellular response, in this case through ROS-mediated proliferation and phenotypic

changes. Therefore, by expanding our class of polymers, we will develop new methods to control cell behavior and health by modulating outside-in cell signaling.

REFERENCES

1. Lutolf MP, Hubbell JA. Synthetic biomaterials as instructive extracellular microenvironments for morphogenesis in tissue engineering. Nat Biotechnol 2005 Jan;23(1):47-55.

2. Sung HJ, Su J, Berglund JD, Russ BV, Meredith JC, Galis ZS. The use of temperature-composition combinatorial libraries to study the effects of biodegradable polymer blend surfaces on vascular cells. Biomaterials 2005 Aug;26(22):4557-4567.

3. Sung HJ, Chandra P, Treiser MD, Liu E, Iovine CP, Moghe PV, et al. Synthetic polymeric substrates as potent pro-oxidant versus anti-oxidant regulators of cytoskeletal remodeling and cell apoptosis. J Cell Physiol 2009 Mar;218(3):549-557.

4. Sung H-J, Luk A, Murthy S, Liu E, Jois M, Joy A, et al. Poly(ethylene glycol) as a sensitive regulator of cell survival fate on polymeric biomaterials: the interplay of cell adhesion and pro-oxidant signaling mechanisms. Soft Matter 2010;6(20):5196-5205.

5. Mani G, Feldman MD, Patel D, Agrawal CM. Coronary stents: A materials perspective. Biomaterials 2007 Mar;28(9):1689-1710.

6. Finn AV, Nakazawa G, Joner M, Kolodgie FD, Mont EK, Gold HK, et al. Vascular responses to drug eluting stents - Importance of delayed healing. Arteriosclerosis Thrombosis and Vascular Biology 2007 Jul;27(7):1500-1510.

7. Onuma Y, Ormiston J, Serruys PW. Bioresorbable Scaffold Technologies. Circulation Journal 2011 Mar;75(3):509-520.

8. Zhang LL, Xiong CD, Deng XM. Biodegradable polyester blends for biomedical application. J Appl Pol Sci 1995;56:103-122.

9. Tang ZG, Black RA, Curran JM, Hunt JA, Rhodes NP, Williams DF. Surface properties and biocompatibility of solvent-cast poly[-caprolactone] films. Biomaterials 2004 Aug;25(19):4741-4748.

10. Bergstrom K, Holmberg K, Safranj A, Hoffman AS, Edgell MJ, Kozlowski A, et al. Reduction of fibrinogen adsorption on PEG-coated polystyrene surfaces. J Biomed Mater Res 1992 Jun;26(6):779-790.

11. Deschamps AA, van Apeldoorn AA, Hayen H, de Bruijn JD, Karst U, Grijpma DW, et al. In vivo and in vitro degradation of poly(ether ester) block copolymers based on poly(ethylene glycol) and poly(butylene terephthalate). Biomaterials 2004 Jan;25(2):247-258.

12. Sun G, Zhang XZ, Chu CC. Effect of the molecular weight of polyethylene glycol (PEG) on the properties of chitosan-PEG-poly(N-isopropylacrylamide) hydrogels. J Mater Sci Mater Med 2008 Aug;19(8):2865-2872.

13. Gimenez S, Ponsart S, Coudane J, Vert M. Synthesis, properties and in vitro degradation of carboxyl-bearing PCL. Journal of Bioactive and Compatible Polymers 2001 Jan;16(1):32-46.

14. Dong CM, Qiu KY, Cu ZW, Feng XD. Synthesis of star-shaped poly(epsilon-caprolactone)-b-poly(DL-lactic acid-alt-glycolic acid) with multifunctional initiator and stannous octoate catalyst. Macromolecules 2001 Jul 3;34(14):4691-4696.

15. Sosnik A, Cohn D. Poly(ethylene glycol)-poly(epsilon-caprolactone) block oligomers as injectable materials. Polymer 2003 Nov;44(23):7033-7042.

16. Sung HJ, Eskin SG, Sakurai Y, Yee A, Kataoka N, McIntire LV. Oxidative stress produced with cell migration increases synthetic phenotype of vascular smooth muscle cells. Ann Biomed Eng 2005 Nov;33(11):1546-1554.

17. Cai H. Hydrogen peroxide regulation of endothelial function: origins, mechanisms, and consequences. Cardiovasc Res 2005 Oct 1;68(1):26-36.

18. Clempus RE, Griendling KK. Reactive oxygen species signaling in vascular smooth muscle cells. Cardiovasc Res 2006 Jul 15;71(2):216-225.

19. Cai H, Harrison DG. Endothelial dysfunction in cardiovascular diseases: the role of oxidant stress. Circ Res 2000 Nov 10;87(10):840-844.

20. Li PF, Dietz R, vonHarsdorf R. Differential effect of hydrogen peroxide and superoxide anion on apoptosis and proliferation of vascular smooth muscle cells. Circulation 1997 Nov 18;96(10):3602-3609.
21. Elahi MM, Kong YX, Matata BM. Oxidative stress as a mediator of cardiovascular disease. Oxid Med Cell Longev 2009 Nov-Dec;2(5):259-269.
22. Su B, Mitra S, Gregg H, Flavahan S, Chotani MA, Clark KR, et al. Redox regulation of vascular smooth muscle cell differentiation. Circ Res 2001 Jul 6;89(1):39-46.
23. Rovner AS, Murphy RA, Owens GK. Expression of smooth muscle and nonmuscle myosin heavy chains in cultured vascular smooth muscle cells. J Biol Chem 1986 Nov 5;261(31):14740-14745.
24. Zanetti M, Zwacka R, Engelhardt J, Katusic Z, O'Brien T. Superoxide anions and endothelial cell proliferation in normoglycemia and hyperglycemia. Arterioscler Thromb Vasc Biol 2001 Feb;21(2):195-200.
25. Galkina E, Ley K. Vascular adhesion molecules in atherosclerosis. Arterioscler Thromb Vasc Biol 2007 Nov;27(11):2292-2301.
26. Sung HJ, Meredith C, Johnson C, Galis ZS. The effect of scaffold degradation rate on three-dimensional cell growth and angiogenesis. Biomaterials 2004 Nov;25(26):5735-5742.
27. Pasche S, Voros J, Griesser HJ, Spencer ND, Textor M. Effects of ionic strength and surface charge on protein adsorption at PEGylated surfaces. Journal of Physical Chemistry B 2005 Sep 22;109(37):17545-17552.
28. Heymann B, Grubmuller H. Elastic properties of poly(ethylene-glycol) studied by molecular dynamics stretching simulations. Chemical Physics Letters 1999 Jul 9;307(5-6):425-432.
29. Hashimoto Y, Yoshinoya S, Aikawa T, Mitamura T, Miyoshi Y, Muranaka M, et al. Enhanced endothelial cell proliferation in acute Kawasaki disease (muco-cutaneous lymph node syndrome). Pediatric Research 1986;20(10):943-946.
30. Newby AC, Zaltsman AB. Molecular mechanisms in intimal hyperplasia. J Pathol 2000 Feb;190(3):300-309.
31. Meurice T, Vallet B, Bauters C, Dupuis B, Lablanche JM, Bertrand ME. Role of endothelial cells in restenosis after coronary angioplasty. Fundam Clin Pharmacol 1996;10(3):234-242.
32. Tajaddini A, Kilpatrick DL, Vince DG. A novel experimental method to estimate stress-strain behavior of intact coronary arteries using intravascular ultrasound (IVUS). J Biomech Eng 2003 Feb;125(1):120-123.